ACS APPLIED MATERIALS & INTERFACES

RESEARCH ARTICLE

www.acsami.org

Sulfonated Poly(arylene ether sulfone ketone) Multiblock Copolymers with Highly Sulfonated Blocks. Long-Term Fuel Cell Operation and Post-Test Analyses

Byungchan Bae,[†] Kenji Miyatake,[*,†,‡] Makoto Uchida,[†] Hiroyuki Uchida,[†,‡] Yoko Sakiyama,[§] Takeou Okanishi,[∥] and Masahiro Watanabe[*,†]

[†]Fuel Cell Nanomaterials Center, and [‡]Clean Energy Research Center, University of Yamanashi, 4 Takeda, Kofu 400-8510

[§]Toray Research Center, Inc., Otsu, Shiga 520-8567,

[∥]Living Environment Development Center, Panasonic Corporation, Moriguchi, Osaka 570-8501, Japan

Supporting Information

ABSTRACT: The stability of poly(arylene ether sulfone ketone) (SPESK) multiblock copolymer membranes having highly sulfonated hydrophilic blocks was tested in an operating fuel cell. The electrochemical properties and drain water were monitored during the test, followed by post-test analyses of the membrane. During a 2000-h fuel cell operation test at 80 °C and 53% RH (relative humidity) and with a constant current density (0.2 A cm^{-2}), the cell voltage showed minor losses, with slight increases in the resistance. In the drain water, anions such as formate, acetate, and sulfate were observed. Post-test analyses of the chemical structure by NMR and IR spectra revealed that the sulfonated fluorenyl group with ether linkage was the most likely to have degraded during the long-term operation, producing these small molecules. The minor oxidative degradation only slightly affected the proton conductivity, water uptake, and phase-separated morphology.

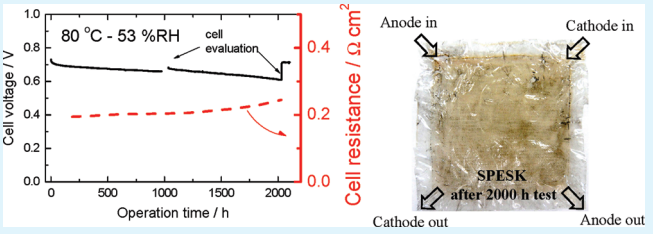

KEYWORDS: poly(arylene ether sulfone ketone)s, ionomers, block copolymer membranes, fuel cells, durability

INTRODUCTION

Perfluorosulfonic acid (PFSA) polymers are state-of-the-art membranes for the polymer electrolyte fuel cell (PEFC). PFSA membranes are composed of a perfluorocarbon backbone with pendant perfluorosulfonic acid groups, which provide robust chemical and physical properties, as well as high proton conductivity. Several types of PFSA membranes, such as Nafion, Flemion, and Aquivion, are commercially available. The differences among these lie in the copolymer composition and the side chain structure and length. Their fully fluorinated chemical structure, however, leads to high production costs and low glass-transition temperatures.

Acid-functionalized aromatic polymers have been studied as alternative ionomer membranes, which include sulfonated poly(arylene ether)s, polyimides, polybenzimidazoles, and polyphenylenes.[1−13] Most of these ionomers contain randomly distributed sulfonic acid groups on the main chains and suffer from low proton conductivity when in a poorly hydrated state (under low relative humidity (RH) conditions). Adequate proton conductivity under low RH conditions is critical for the PEFC membranes, since a minimal size of the balance of plant (BOP), achievable if external humidification is not required, is beneficial for practical fuel cell operation. Fuel cell operation at high temperature and low RH could potentially help to realize a highly efficient, cost-effective PEFC. Recently, there has been significant improvement in aromatic ionomer membranes. Block copolymer architecture and incorporation of highly sulfonated or acidic moieties has resulted, to a great extent, in highly developed hydrophilic/hydrophobic nanophase separation and improved proton conductivities at high temperature and low RH.[14−17] Some membranes have shown fuel cell performance comparable to that of Nafion under low RH conditions.[18,19]

Durability is another important issue for nonfluorinated aromatic ionomer membranes. The carbon−hydrogen bonds are often susceptible to hydrogen abstraction reactions by highly oxidizing OH radicals, and the electron-rich ether and aromatic groups are more likely to be oxidized than C−F bonds. These undesirable reactions appear to be occurring during fuel cell operation; however, detailed studies on the stability and degradation mechanism under fuel cell operation are few. There have been reports on the stability of aromatic ionomer membranes or their model compounds by ex situ methods.[20−23] Fenton's test is most commonly used for evaluating oxidative stability; in this test, no aromatic ionomer membranes are able to compete with the PFSA membranes. Nevertheless, sulfonated polyimide and poly(arylene ether) membranes have been found to survive 5000 h PEFC operation tests.[24−26] These results suggest that accelerated

Received: May 10, 2011
Accepted: June 27, 2011
Published: June 27, 2011

dx.doi.org/10.1021/am200579z | ACS Appl. Mater. Interfaces 2011, 3, 2786–2793

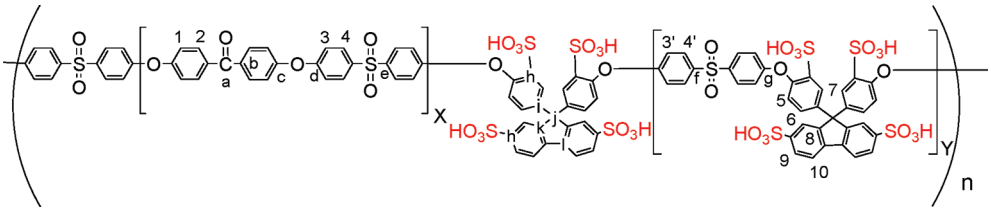

Figure 1. Chemical structure of SPESK multiblock copolymers.

ex situ tests, such as Fenton's test, are not appropriate to predict the durability of aromatic ionomer membranes in operating fuel cells. One of the reasons is that the gas permeabilities of membranes and the effects of electrocatalysts are not taken into account. Therefore, in situ degradation should be more carefully investigated for alternative ionomer membranes. Recently, Ericson et al. investigated structural changes of their sulfonated styrene-grafted poly(vinylidene fluoride) membrane after a 500 h fuel cell operation test by use of confocal micro-Raman spectroscopy.[27] They concluded that the degradation of the membrane was accelerated on the cathode side. Thinning of the membrane was also confirmed.[28] More recently, Perrot et al. investigated their sulfonated poly(arylene ether ketone) membrane under both ex situ and fuel cell operating conditions.[29] Their research was informative in predicting the durability of hydrocarbon-based membranes.

Recently, we synthesized a series of sulfonated multiblock poly(arylene ether sulfone ketone)s (SPESKs) (Figure 1) with highly sulfonated hydrophilic blocks.[30] The membranes showed distinct hydrophilic/hydrophobic phase separation, due to their unique block structure, and therefore high proton conductivity under a wide range of RH conditions. An H_2/air fuel cell was successfully operated with the SPESK membrane at 100 °C and 30% RH.[19] In our previous papers, the synthesis, physical properties, and fuel cell performance of the SPESK membranes have been reported.[31,32] In this article, we report long-term fuel cell operation of the SPESK membrane. During the cell operation, the electrochemical performance was monitored, and the drain water was analyzed. The post-test analyses of the membrane were conducted via NMR and IR spectra, GPC measurements, proton conducting properties, and microscopic observations. The combination of in situ and post-test analyses provide new insight into the degradation of aromatic ionomer membranes in operating fuel cells.

EXPERIMENTAL SECTION

Materials. The SPESK membrane was synthesized as described previously.[19,31] The degree of polymerization of the hydrophobic (X) and hydrophilic blocks (Y) was controlled to be 30 and 8, respectively. The ion exchange capacity (IEC) of SPESK X30Y8 was determined by titration to be 1.7 mequiv g^{-1}. Carbon-supported Pt−Ru and Pt−Co catalysts, TEC61E54 and TEC36F52, were purchased from Tanaka Kikinzoku Kogyo.

Long-Term Fuel Cell Test and In situ Analysis of MEAs. A membrane-electrode assembly (MEA) with an SPESK-membrane (30 μm thick) and 36 cm^2 electrode area was operated at 80 °C and 53% RH under ambient pressure. Pt−Ru anode and Pt−Co cathode catalysts were used to prepare the respective electrodes with loading amounts of 0.3 and 0.6 mg cm^{-2}, respectively. Mixed gas (75% hydrogen -25% carbon dioxide) was supplied to the anode with 70% H_2 utilization. For the cathode, air was supplied with 40% O_2 utilization. The cell voltage and ohmic resistance during the long-term test were monitored by use of a digital AC milliohm tester (MODEL3566, Tsuruga Electric Co.).

The catalyst layers were examined during the long-term test with cyclic voltammograms (CVs) measured by a potentiostat (HZ-3000, Hokuto-Denko). For the CV measurement of the cathode, the cathode compartment was purged with N_2 (300 mL min^{-1}, 53% RH), while H_2 gas (300 mL min^{-1}, 53% RH) was supplied to the anode. Prior to the potential sweep, the potential was held at the rest potential for 30 s. Then, the potential was swept between 0.10 and 1.00 V at 10 mV s^{-1}. The electrochemically active surface area (ECA) was estimated from the hydrogen adsorption charge ΔQ_H in the negative-going potential scan, referred to $\Delta Q_H^\circ = 0.21$ mC cm^{-2}, the value adopted conventionally for clean polycrystalline platinum.[33,34] The current at 0.40 V was subtracted as a background current. The amount of hydrogen crossing over from the anode to the cathode was tested by gas chromatography (GC-8A, Shimadzu Co.). Hydrogen and nitrogen were supplied at 300 mL min^{-1} to the anode and the cathode, respectively.

Drain water from the both electrodes was collected periodically during the test, and the chemical species in the water were analyzed by ion chromatography (IC) and total organic carbon (TOC) analysis. The concentrations of anions were analyzed by a Dionex ICS-3000 system with an Ion Pac AS18 column and KOH gradient eluent. A Dionex DX-500 system with an Ion Pac AS12A column and $NaCO_3$−$NaHCO_3$ mixed eluent were used for the analysis of other ions. The TOC in the aqueous solution was measured by a Total Organic Carbon analyzer (Toray Engineering TNC-6000).

Post-Test Analyses of SPESK Membrane. After the 2000 h fuel cell test, the MEA was humidified at 100% RH and 80 °C for 100 h in order to drain the chemical species remaining in the catalyst layer. Then, the MEA was dissembled carefully for post-test analyses. The detached SPESK membrane was cut into several pieces and analyzed as shown in Figure S1 in the Supporting Information.

The ion exchange capacity (IEC) of the SPESK membrane was investigated by back-titration before and after the test. A piece of SPESK membrane was equilibrated overnight in a large excess of saturated NaCl aqueous solution. The HCl released by ion exchange was titrated with a standard 0.01 M NaOH aqueous solution. Water uptake and proton conductivity of the membrane were measured before and after the test, as previously reported.[35] The molecular weight was measured by gel permeation chromatography (GPC) equipped with two TOSOH TSK-gel GMHHR-H and GMHHR-M columns and a Showa Denko RI-71 refractive index detector, with DMAc containing 0.05 M LiCl as the eluent. The molecular weight was calibrated with standard polystyrene samples. ^{1}H and ^{13}C NMR spectra were obtained on a Varian UNITY INOVA 500 using deuterated dimethyl sulfoxide (DMSO-d_6) as a solvent and tetramethylsilane (TMS) as an internal reference. ATR-FTIR spectra of the membranes were analyzed with an FTS-55A (Bio-Rad Digilab) spectrometer. For transmission electron microscopic (TEM) observations, the sulfonic acid groups of the membranes were stained with lead ions by immersing them overnight in 0.5 M lead acetate aqueous solution, rinsing with deionized water, and drying in a vacuum oven for 12 h. The stained membranes were embedded in epoxy resin, sectioned to 90 nm thickness with a Leica microtome Ultracut UCT, and

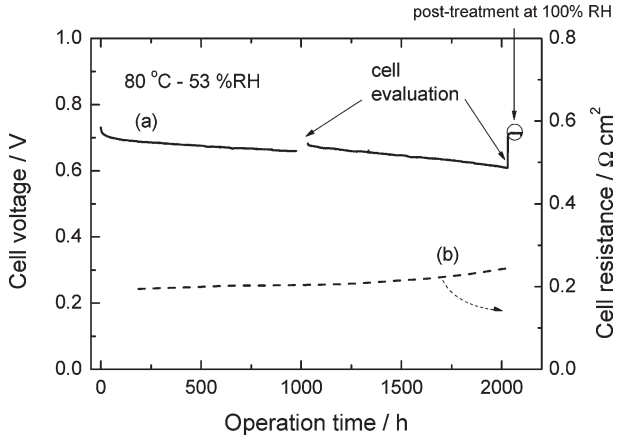

Figure 2. Time course of (a) cell voltage at 0.2 A cm^{-2} and (b) cell resistance of a fuel cell with the SPESK membrane. The fuel cell was operated with 75% H_2/25% CO_2 (anode) and air (cathode) at 80 °C and 53% RH.

images were taken on a Hitachi HD-2300C STEM with an accelerating voltage of 200 kV. A Shimazu EPMA-1600 was used for scanning electron microscopy (SEM) and electron probe microanalysis (EPMA) to analyze the cross-sectional images of the membranes and elemental distributions through the membranes, respectively. Laser ablation inductively coupled plasma mass spectrometry (LA-ICP-MS) analyses were carried out using a Perkin-Elmer ICP-MS coupled with an ESI Japan New Wave Research UP213 Nd:YAG laser. Detailed ICP-MS analyses were conducted with an Agilent 4500.

An H_2O_2 vapor exposure experiment was conducted as previously reported.[36] The temperature of the chamber for the H_2O_2 vapor exposure was controlled at 90 °C. Nitrogen gas humidified with 1 wt % hydrogen peroxide aqueous solution was mixed with dry nitrogen to achieve a humidity of 30% RH, and this gas stream was supplied to the chamber. Samples were exposed to the H_2O_2 vapor for 100 h. The oxidative products contained in the outlet gas were captured with 100 mL of 1 mM KOH aqueous solution.

RESULTS AND DISCUSSION

Long-Term Fuel Cell Operation of SPESK MEA. The MEA with SPESK membrane (30 μm thick) was operated in a fuel cell for 2000 h at a constant current density of 0.2 A cm^{-2} at 80 °C and 53% RH. To simulate practical fuel cell systems with hydrogen reformers, 75% hydrogen/25% carbon dioxide, and air were supplied to the anode and cathode, respectively. The cell voltage and resistance are plotted as a function of operation time in Figure 2. The high proton conductivity of the SPESK membrane resulted in a relatively high cell voltage, about 0.7 V. This cell voltage was much higher than that for our randomly sulfonated polyimide (0.5 V) and poly(arylene ether) (0.45 V) under similar operating conditions.[25,37] The cell voltage decreased with time during operation, and the average decay rate was ca. 43 μV h^{-1}. The cell voltage recovered to some extent during the performance evaluation after 1000 h operation. The performance evaluation included I−V and OCV measurements, H_2 cross-leak test, and cyclic voltammetry (CV), all of which help to remove water-soluble adsorbates from the catalyst, leading to performance recovery by redistribution of water within the MEA. Finally, the constant current density operation was stopped at 2000 h, followed by a 100 h postoperation period at 100% RH in order to remove water-soluble residues (possible decomposition products) from the MEA.

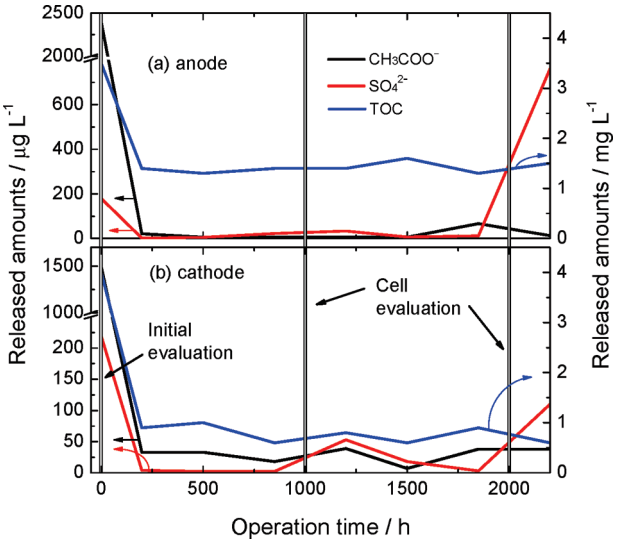

Figure 3. Amounts of acetate and sulfate anions released and TOC from (a) anode and (b) cathode as a function of fuel cell operation time. The left vertical axis represents acetate and sulfate anions, and the right axis represents TOC.

The ohmic resistance of the cell was nearly constant (0.20 Ω cm^2) up to 1000 h and then increased slightly. The final value of the resistance was 0.24 Ω cm^2 at 2000 h. The cell was disassembled for post-test analyses of the membrane.

In situ Analyses of SPESK MEA during Long-Term Fuel Cell Operation. During the long-term fuel cell operation, drain water was sampled both from the anode and the cathode and was analyzed by ion chromatography (IC) and total organic carbon (TOC) measurements. The results are summarized in Tables S1 and S2 in the Supporting Information. Acetate and sulfate ions were the main detected anions. The amounts of the anions released are plotted, along with measured TOC values, as a function of operation time in Figure 3.

At the initial evaluation (prior to the long-term operation), the largest amounts of acetate and sulfate ions were detected both from the anode and the cathode. It can reasonably be assumed that the acetate ion was the degradation product of *N,N*-dimethylacetamide (DMAc), which had been used as the casting solvent and could have remained in the membrane. Apparently, drying in a vacuum and washing with water several times did not complete the removal of this high-boiling-point solvent. The possible degradation mechanism of DMAc involves (1) acid-catalyzed hydrolysis and (2) oxidation. The former reaction is catalyzed by the sulfonic acid groups in the SPESK as follows

$$CH_3CON(CH_3)_2 + H_2O + H^+ \rightarrow CH_3COOH + (CH_3)_2NH_2^+ \quad (1)$$

The latter reaction could take place electrochemically at the surface of the electrocatalysts (Pt−Ru at the anode and Pt−Co at the cathode). We observed a gradual increase in the electrochemically active surface area (ECA) at the initial stage of potential cycling. The lower ECA at the very beginning might be due to the poisoning of the catalyst by DMAc adsorption.

Similar to the situation for the acetate ions, the initial release of sulfate ions probably originated from residual sulfuric acid in the

Table 1. Quantitative Analysis of Sulfate Ions in the Drain Water from Both Electrodes and Comparison with Initial Amount of Sulfonic Acid Groups

	sulfate ions from the anode				sulfate ions from the cathode					
collection time	collected drain water (g)	concentration (μg L^{-1})	amount (μg)	accumulated amount (μg)	collected drain water (g)	concentration (μg L^{-1})	amount (μg)	accumulated amount (μg)	total accumulated amount[a] (μg)	accumulated loss of sulfonic acid groups[b] (%)
initial evaluation	303	180	55	55	2002	220	440	440	495	2.0
0−200 h	367	2	1	56	1936	4	8	448	504	2.1
200−500 h	506	5	2	58	3121	0	0	448	506	2.1
500−850 h	512	22	11	69	3163	0	0	448	517	2.1
850−1200 h	563	33	19	88	3124	53	166	614	702	2.9
1200−1500 h	507	7	4	92	3175	18	57	671	763	3.1
1500−1850 h	512	12	6	98	3199	3	10	681	779	3.2
1850−2200 h	585	760	444	542	2719	110	299	980	1522	6.2

[a] Sum of anode and cathode side. [b] Accumulated loss of sulfonic acid groups (%) = (total accumulated amount of released sulfate ion in mol from both electrodes)/(total amount of sulfonic acid in the original membrane in mol) × 100. The amount of sulfonic acid groups in the original membrane was calculated from IEC (1.7 mequiv g^{-1}), density (1.4 g cm^{-3}), area (36 cm^2), and thickness (30 μm).

membrane, which was used for the acidification in the final process of the membrane preparation. Because the amount of sulfate is a crucial parameter for evaluating membrane degradation, the total amount of sulfate released at each collection time was quantified and compared with the total amount of sulfonic acid groups in the original SPESK membrane in Table 1. At the time of the initial cell evaluation, the amount of sulfate released accounted for ca. 2% of the sulfonic acid groups in the membrane. Because the membrane is unlikely to degrade in such a short time, it was assumed that the initial release of sulfate ions was from the residual sulfuric acid within the original membrane.

During the long-term fuel cell operation at constant current density, a steady but low-level release of acetate and sulfate ions was observed from the both electrodes. These anions could be associated with the degradation of the membrane. Perrot et al. reported a release of alkyl carboxylic acid via a phenol species when their sulfonated model compounds, poly(arylene ether ketone) oligomers, were exposed to H_2O_2 aqueous solution.[23] They proposed that ether linkages in the vicinity of sulfonic acid groups can be oxidized by hydroxyl radicals. The SPESK membrane in the present report appears to have experienced a similar degradation route. The acetate and sulfate ions released during the fuel cell operation could result from the oxidative degradation of the hydrophilic blocks. The total amount of sulfate ions released during the 2000 h test accounted for merely 4.2% of the sulfonic acid groups contained in the SPESK membrane, under the assumption that the initial release of sulfate ions (2.0%) was from the sulfuric acid contaminant. Details are discussed below in the section on post-test analyses of the membrane.

The electrochemical properties of the SPESK MEA were also investigated as part of the performance evaluations during the long-term test. Figure 4 shows CV curves of the anode and cathode obtained at 0, 1000, and 2000 h operation, respectively. Other parameters for the SPESK MEA are included in Table 2. The shapes of CV curves were different comparing the anode (Pt−Ru) and the cathode (Pt−Co). The ECA values decreased with operation time, and the decrease was severer for the anode than for the cathode. The decrease in ECA would be ascribed to the degradation of the catalyst, e.g., dissolution and agglomeration

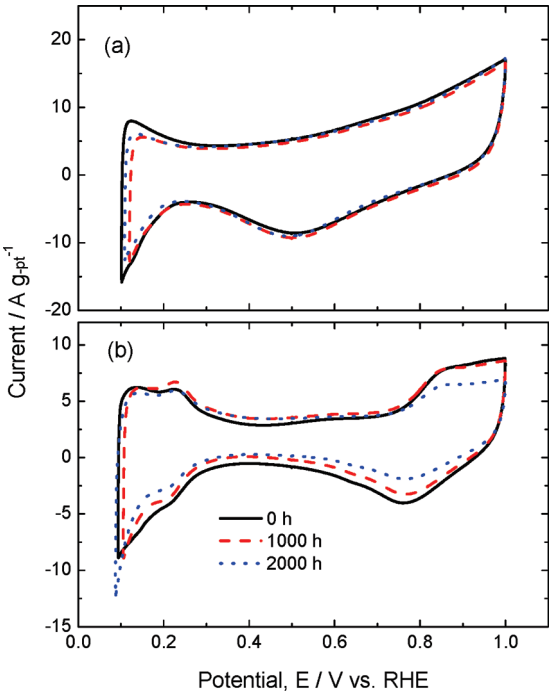

Figure 4. Cyclic voltammograms of (a) anode and (b) cathode at 0 h (initial), 1000 h, and 2000 h operation.

of nanoparticles. The growth of catalyst particles during long-term testing of Nafion-based MEAs has been reported to cause lowered fuel cell performance.[38,39] In addition to the ECA, the oxide formation charge (Q_{oxide}) in the 0.4 − 1.0 V region decreased in the cathode during the 2000 h fuel cell operation. Accordingly, the mass activity (MA) at 0.9 V also decreased. Since the decrease of Q_{oxide} was greater than that of ECA, it is considered that some anionic species were specifically adsorbed onto the cathode catalyst at high potential. We have previously found that the specific adsorption of sulfate ions on the surface of Pt particles affected Q_{oxide} but not ECA.[40] The Pt−Co catalyst also appeared to have experienced a similar poisoning from

Table 2. Electrochemical Parameters during Performance Evaluations of SPESK MEA at 0, 1000, and 2000 h

evaluation	0 h	1000 h	2000 h
cell voltage (V)[a]	0.716	0.699	0.667
resistance (Ω cm^2)[a]	0.187	0.193	0.216
OCV (V)	1.016	1.005	1.012
H_2 crossover (%)[b]	0.05	0.13	0.15
MA at 0.9 V (A g^{-1})	38	27	21
Q_{oxide} of anode (C g^{-1})	293	284	290
Q_{oxide} of cathode (C g^{-1})	127	108	72
ECA of anode/m^2 g^{-1}	19.8	16.3	13.3
ECA of cathode (m^2 g^{-1})	35.7	34.6	29.2

[a] During performance evaluation at 0.2 A cm^{-2}. [b] Molar percentage of hydrogen crossing over from the anode to the cathode (300 mL min^{-1} hydrogen and nitrogen at anode and cathode, respectively).

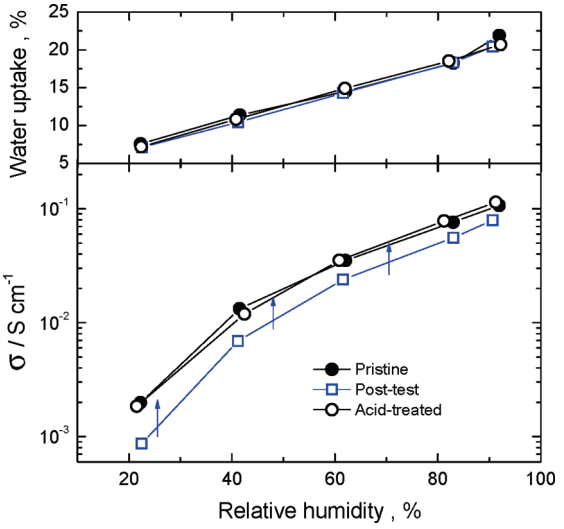

Figure 5. Water uptake and proton conductivity (σ) of pristine, post-test, and acid-treated membranes at 80 °C as a function of RH.

degradation products of the membrane such as acetate and sulfate. In contrast, the Pt−Ru catalyst in the anode showed little change in Q_{oxide}. The results are surprising due to the fact that similar amounts of degradation products were found in the water drained from both anode and cathode. At present, we do not have a conclusive explanation for this. One plausible reason is that the specific adsorbability of anions is different on Pt−Co and Pt−Ru under the acidic conditions.

It should be noted that hydrogen crossover (permeation) through the membrane increased with operation time. The increase of the hydrogen permeability indicates membrane degradation; however, it was minor, as confirmed by the very small changes in the open circuit voltage (OCV).

Post-Test Analyses of the SPESK Membrane. After 2000 h fuel cell operation, the membrane was carefully removed from the gas diffusion electrodes and subjected to analysis. Figure S1 in the Supporting Information shows the SPESK membrane after the test. The membrane was slightly brown-colored but retained its flexibility and toughness. It was cut into several pieces for the post-test analyses. First, proton conductivity and water uptake of the SPESK membrane were measured because the cell resistance increased slightly after 1500 h, as shown in Figure 2. Figure 5 compares the humidity dependence of the proton conductivity and water uptake at 80 °C between pristine and post-test membranes. The post-test membrane showed water uptake behavior similar to that for the pristine one over the entire humidity range, indicating that they had similar hydrophilicity. In contrast, the post-test membrane showed somewhat lower proton conductivity. For example, its conductivity was 0.007 S cm^{-1} at 40% RH, which was about half that of the pristine membrane. The IEC value of the post-test membrane (1.45 mequiv g^{-1}) was lower than that of the pristine one (1.75 mequiv g^{-1}). By treating it in 1 M aqueous sulfuric acid solution, the post-test membrane showed comparable IEC (1.73 mequiv g^{-1}) and proton conductivity to those of the pristine membrane. These results imply that the decrease in IEC and proton conductivity cannot be ascribed to membrane degradation but to ionic contamination of the sulfonic acid groups, possibly from the humidified gases flowing through metal tubing and end-plates. Taking the totally released amount of sulfate ions (Table 1) into account, this recovery is reasonable. Analyses of the drain water allowed us to estimate that the loss of sulfonic acid groups from the membrane was 4.2% (= 6.2 − 2.0), which is consistent with the very minor changes in water uptake, IEC, and proton conductivity of the acid-treated post-test membrane.

Table 3. Molecular Weights of Pristine and Post-Test SPESK Membranes

sample	M_n[a]	M_w[a]	PI (M_w/M_n)
pristine	84.6	193.0	2.3
cathode inlet	44.4	90.6	2.0
cathode outlet	56.8	130.0	2.3
anode inlet	46.2	98.5	2.1
anode outlet	58.1	137.0	2.4
anode outlet (acid-treated)	58.0	136.9	2.4

[a] Molecular weights in kDa.

The molecular weight of the post-test SPESK was measured by GPC at four different positions (inlet and outlet of the anode and cathode sides, respectively). Table 3 summarizes the number-averaged molecular weight (M_n), weight-averaged molecular weight (M_w), and molecular weight distribution (polydispersity index; PI = M_w/M_n) of the post-test membrane (see Figure S2 in the Supporting Information for the elution curves). The molecular weights of the post-test membrane were lower than those of the pristine membrane, regardless of their sampling positions. We examined the effect of ionic contamination on the GPC profiles with the post-test sample taken from the anode outlet because radii of gyration of the SPESK would differ by the kinds of counter cations. As shown in Figure S3 in the Supporting Information, acid treatment did not alter the GPC curve of the post-test membrane, indicating that the effect of minor contamination of possible cationic species was negligible. The decrease in molecular weight was somewhat more significant at the gas inlet (ca. 55%) compared with the outlet (ca. 42%). Because the SPESK membrane is stable to hydrolysis, as we have proved previously,[31] the main degradation mode would be oxidation by hydrogen peroxide and radical species derived therefrom. The oxygen and hydrogen concentrations (or partial pressures) were higher at the inlet than the outlet, and therefore the amounts of crossover gases and generated hydrogen peroxide should be greater at the inlet. The PIs of the post-test membrane ranged between 2.0 and 2.4 and were comparable to that of the pristine

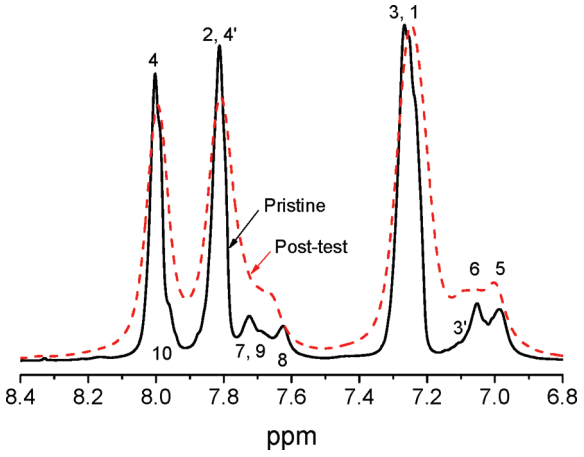

Figure 6. ^{1}H NMR spectra of the pristine and post-test SPESK membranes.

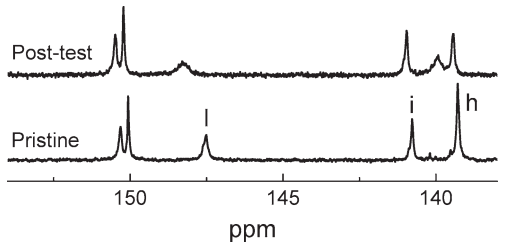

Figure 7. ^{13}C NMR spectra of the pristine and post-test SPESK membranes.

one (2.3). The results suggest that the degradation was not significant and thus not of the chain reaction (not unzipping mechanisms as the case for PFSA membranes). Compared with the ex situ oxidative stability results,[31] the SPESK membrane showed rather good stability during the practical fuel cell operation. The lower gas permeability of the SPESK membrane should be responsible for producing lower amounts of hydrogen peroxide during fuel cell operation.

The post-test membrane was then analyzed by ^{1}H and ^{13}C NMR spectra. The ^{1}H NMR spectra were compared between pristine and post-test membranes in Figure 6 (refer to Figure 1 for assignments). Although the spectrum was broader for the post-test membrane, the integral ratios of the peaks were comparable with those of the pristine membrane. The broadening of the peaks could be related to the minor ionic contamination and/or ionic cross-linking. The ^{13}C NMR spectra (Figure 7 and Figure S4 in the Supporting Information) were more informative in analyzing the degradation mechanism. The relative intensity of peak 'h' compared to 'i' was smaller, and a new peak was observed at 140 ppm for the post-test membrane. Peak 'l' for the fluorenyl carbon shifted to lower magnetic field. The ^{13}C NMR data suggest structural changes in the sulfonic acid-containing fluorenyl groups. IR spectra were also compared between pristine and post-test membranes in Figure S5 in the Supporting Information. The spectra were normalized to the peak at 1585 cm^{-1}, which was assigned to the aromatic C═C vibration. There were practically no differences observed, except for the peak for the C−H vibration at 1150 cm^{-1}: the post-test membrane showed a lower peak intensity.

Table 4. Analysis of Drain Water During H_2O_2 Vapor Exposure of a Precursor of the Hydrophilic Oligomer

	concentrations of detected ions (μg g^{-1})		
chemical species	0−22 h	22−44 h	44−66 h
acetate	240	220	180
formate	350	200	120
oxalate	17	12	16
TOC	530	430	360

The combination of these NMR and IR data led to the idea that the degradation of the SPESK membrane occurred at the fluorenyl groups in the hydrophilic blocks. There were no indications of degradation in the hydrophobic blocks. It can be assumed that the oxidative degradation of the sulfonated fluorenyl biphenylene groups produced the sulfate and acetate ions. In order to confirm this assumption, a precursor for the hydrophilic oligomer was chosen as a model compound (see Figure S6 in the Supporting Information for chemical structure) and was subjected to an accelerated oxidative stability test, in which the sample was exposed to H_2O_2 vapor.[36] The ionic species detected and their concentrations are summarized in Table 4. Acetate and formate ions were detected as the major degradation products. Although the degradation of the oligomer was very slight, these data support the above assumption. Because no intermediate products were detected, the degradation mechanism of the hydrophilic blocks could not be interpreted. In the literature, it has been reported that the carbon atoms ortho to ether linkages (for example, the 1, 3, 3′, and 5 positions in Figure 1) are susceptible to oxidation due to the increased electron density.[29,41,42] In addition, the sulfonic acid groups should facilitate the oxidation of the vicinal aromatics by hydrophilic H_2O_2 and radicals. It is therefore reasonably considered that the 3′, 5 and l positions in Figure 1 are the most probable sites at which the oxidative degradation of the hydrophilic blocks may be initiated.

Figure 8 shows TEM images of the lead-ion exchanged pristine and post-test SPESK membranes. The dark spots represent ion-exchanged hydrophilic clusters, and the light ones represent hydrophobic parts. The pristine membrane showed well-developed phase separation between hydrophilic and hydrophobic blocks, as previously reported.[31] The post-test sample taken near the cathode showed a similar phase-separated morphology. In contrast, such characteristic morphology was less pronounced for a sample taken near the anode, with a somewhat blurred interface between hydrophilic and hydrophobic domains. This is probably due to a decreased concentration of sulfonic acid groups. In the last stage of the fuel cell operation, a greater amount of sulfate ions was released in the drain water from the anode than from the cathode, as shown in Figure 3 and Table 1. The membrane degradation thus appears to have been more severe at the anode side than at the cathode side.

Cross-sectional SEM and EPMA images of the post-test membrane are compared with those of the pristine one in Figure S7 in the Supporting Information. The membrane thickness and the contents of carbon and sulfur and their distributions did not change noticeably after the fuel cell operation. In addition, there was no evidence of the formation of Pt particles (or Pt band) in the post-test membrane, which are often observed for perfluorinated ionomer membranes and thus directly show evidence of catalyst degradation. The results suggest that the degradation of

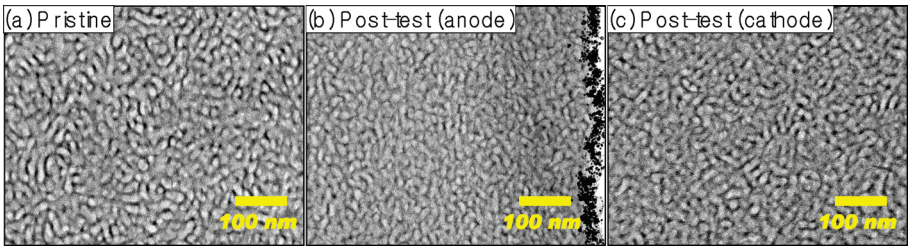

Figure 8. TEM images of lead ion-stained (a) pristine and post-test SPESK membranes, taken (b) near the anode and (c) near the cathode.

the membrane and catalyst was negligible. Very small amounts (<40 ppm) of metal ions such as Li, Na, K, Ca, Cr, Fe, Co, Cu, Ru, and Pt, were detected in the membrane by the LA-ICP-MS and ICP-MS analyses. These ions were indicators of minor degradation of the catalysts and contamination from the stainless steel tubing used for humidification and from the environment.

CONCLUSIONS

The long-term stability of the SPESK multiblock copolymer membrane was tested under fuel cell operation at a current density 0.2 A cm^{-2} at 53% RH and 80 °C for 2000 h. While the membrane maintained the original IEC, water affinity, and proton conductivity, minor oxidative degradation occurred in the hydrophilic blocks. The phenylene rings with electron-donating ether linkages, because of their high electron density, were most likely to be attacked by hydrogen peroxide and derived radicals. The major decomposition products were acetate, formate, and sulfate anions, which were adsorbed onto the catalysts to cause degradation in fuel cell performance. The hydrophobic blocks were robust and did not show degradation. The results suggest that hydrophilic blocks with lower electron density should be designed to improve the durability of the multiblock aromatic ionomer membranes.

ASSOCIATED CONTENT

Supporting Information. Analysis of drain water from both anode and cathode during the long-term test. Photograph, GPC, NMR, SEM/EPMA images, and IR data of the post-test membrane. This material is available free of charge via the Internet at http://pubs.acs.org.

AUTHOR INFORMATION

Corresponding Author

*Tel: +81 55 220 8707 (K.M.); +81 55 254 7091 (M.W.). E-mail: miyatake@yamanashi.ac.jp (K.M.); m-watanabe@yamanashi.ac.jp (M.W.).

ACKNOWLEDGMENT

The authors acknowledge the Kaneka Corporation for supplying the SPESK membranes. This work was partly supported by the New Energy and Industrial Technology Development Organization (NEDO) through the "Research on Nanotechnology for High Performance Fuel Cells" (HiPer-FC) project, and the Ministry of Education, Culture, Sports, Science and Technology (MEXT) Japan through a Grant-in-Aid for Scientific Research (20350086).

REFERENCES

(1) Wang, F.; Hickner, M.; Kim, Y. S.; Zawodzinski, T. A.; McGrath, J. E. *J. Membr. Sci.* **2002**, *197*, 231–242.
(2) Chikashige, Y.; Chikyu, Y.; Miyatake, K.; Watanabe, M. *Macromolecules* **2005**, *38*, 7121–7126.
(3) Xing, P.; Robertson, G. P.; Guiver, M. D.; Mikhailenko, S. D.; Wang, K.; Kaliaguine, S. *J. Membr. Sci.* **2004**, *229*, 95–106.
(4) Gil, M.; Ji, X.; Li, X.; Na, H.; Hampsey, J. E.; Lu, Y. *J. Membr. Sci.* **2004**, *234*, 75–81.
(5) Shang, X.; Tian, S.; Kong, L.; Meng, Y. *J. Membr. Sci.* **2005**, *266*, 94–101.
(6) Miyatake, K.; Zhou, H.; Matsuo, T.; Uchida, H.; Watanabe, M. *Macromolecules* **2004**, *37*, 4961–4966.
(7) Yin, Y.; Suto, Y.; Sakabe, T.; Chen, S.; Hayashi, S.; Mishima, T.; Yamada, O.; Tanaka, K.; Kita, H.; Okamoto, K.-i. *Macromolecules* **2006**, *39*, 1189–1198.
(8) Gao, Y.; Robertson, G. P.; Kim, D.-S.; Guiver, M. D.; Mikhailenko, S. D.; Li, X.; Kaliaguine, S. *Macromolecules* **2007**, *40*, 1512–1520.
(9) Vallejo, E.; Pourcelly, G.; Gavach, C.; Mercier, R.; Pinéri, M. *J. Membr. Sci.* **1999**, *160*, 127–137.
(10) Wainright, J. S.; Wang, J.-T.; Weng, D.; Savinell, R. F.; Litt, M. *J. Electrochem. Soc.* **1995**, *142*, L121–L123.
(11) Jones, D. J.; Roziere, J. *J. Membr. Sci.* **2001**, *185*, 41–58.
(12) Fujimoto, C. H.; Hickner, M. A.; Cornelius, C. J.; Loy, D. A. *Macromolecules* **2005**, *38*, 5010–5016.
(13) Yang, Y.; Siu, A.; Peckham, T. J.; Holdcroft, S. *Adv. Polym. Sci.* **2008**, *215*, 55–126.
(14) Miyatake, K.; Chikashige, Y.; Higuchi, E.; Watanabe, M. *J. Am. Chem. Soc.* **2007**, *129*, 3879–3887.
(15) Roy, A.; Yu, X.; Dunn, S.; McGrath, J. E. *J. Membr. Sci.* **2009**, *327*, 118–124.
(16) Matsumura, S.; Hlil, A. R.; Lepiller, C.; Gaudet, J.; Guay, D.; Shi, Z.; Holdcroft, S.; Hay, A. S. *Macromolecules* **2008**, *41*, 281–284.
(17) Mikami, T.; Miyatake, K.; Watanabe, M. *ACS Appl. Mater. Interfaces* **2010**, *2*, 1714–1721.
(18) Einsla, M. L.; Kim, Y. S.; Hawley, M.; Lee, H.-S.; McGrath, J. E.; Liu, B.; Guiver, M. D.; Pivovar, B. S. *Chem. Mater.* **2008**, *20*, 5636–5642.
(19) Bae, B.; Yoda, T.; Miyatake, K.; Uchida, H.; Watanabe, M. *Angew. Chem., Int. Ed.* **2010**, *49*, 317–320.
(20) Meyer, G.; Gebel, G.; Gonon, L.; Capron, P.; Marscaq, D.; Marestin, C.; Mercier, R. *J. Power Sources* **2006**, *157*, 293–301.
(21) Meyer, G.; Perrot, C.; Gebel, G.; Gonon, L.; Morlat, S.; Gardette, J.-L. *Polymer* **2006**, *47*, 5003–5011.
(22) Schönberger, F.; Kerres, J.; Dilger, H.; Roduner, E. *Phys. Chem. Chem. Phys.* **2009**, *11*, 5782–5795.
(23) Perrot, C.; Gonon, L.; Bardet, M.; Marestin, C.; Pierre-Bayle, A.; Gebel, G. *Polymer* **2009**, *50*, 1671–1681.
(24) Asano, N.; Aoki, M.; Suzuki, S.; Miyatake, K.; Uchida, H.; Watanabe, M. *J. Am. Chem. Soc.* **2006**, *128*, 1762–1769.
(25) Aoki, M.; Chikashige, Y.; Miyatake, K.; Uchida, H.; Watanabe, M. *Electrochem. Commun.* **2006**, *8*, 1412–1416.
(26) Borup, R.; Meyers, J.; Pivovar, B.; Kim, Y. S.; Mukundan, R.; Garland, N.; Myers, D.; Wilson, M.; Garzon, F.; Wood, D.; Zelenay, P.; More, K.; Stroh, K.; Zawodzinski, T.; Boncella, J.; McGrath, J. E.; Inaba, M.; Miyatake, K.; Hori, M.; Ota, K.; Ogumi, Z.; Miyata, S.; Nishikata, A.;

Siroma, Z.; Uchimoto, Y.; Yasuda, K.; Kimijima, K.-i.; Iwashita, N. *Chem. Rev.* **2007**, *107*, 3904–3951.
(27) Ericson, H.; Kallio, T.; Lehtinen, T.; Mattsson, B.; Sundholm, G.; Sundholm, F.; Jacobsson, P. *J. Electrochem. Soc.* **2002**, *149*, A206–A211.
(28) Gode, P.; Ihonen, J.; Strandroth, A.; Ericson, H.; Lindbergh, G.; Paronen, M.; Sundholm, F.; Sundholm, G.; Walsby, N. *Fuel Cells* **2003**, *3*, 21–27.
(29) Perrot, C.; Gonon, L.; Marestin, C.; Morin, A.; Gebel, G. *J. Power Sources* **2010**, *195*, 493–502.
(30) Bae, B.; Miyatake, K.; Watanabe, M. *ACS Appl. Mater. Interfaces* **2009**, *1*, 1279–1286.
(31) Bae, B.; Miyatake, K.; Watanabe, M. *Macromolecules* **2010**, *43*, 2684–2691.
(32) Bae, B.; Yoda, T.; Miyatake, K.; Uchida, M.; Uchida, H.; Watanabe, M. *J. Phys. Chem. B* **2010**, *114*, 10481–10487.
(33) Watanabe, M.; Motoo, S. *J. Electroanal. Chem.* **1975**, *60*, 259–266.
(34) Watanabe, M.; Motoo, S. *J. Electroanal. Chem.* **1975**, *60*, 275–283.
(35) Bae, B.; Miyatake, K.; Watanabe, M. *Macromolecules* **2009**, *42*, 1873–1880.
(36) Takasaki, M.; Nakagawa, Y.; Sakiyama, Y.; Tanabe, K.; Ookubo, K.; Sato, N.; Minamide, T.; Nakayama, H.; Hori, M. *ECS Transactions* **2009**, *17*, 439–447.
(37) Aoki, M.; Asano, N.; Miyatake, K.; Uchida, H.; Watanabe, M. *J. Electrochem. Soc.* **2006**, *153*, A1154–A1158.
(38) Xie, J.; Wood, D. L.; Iii; More, K. L.; Atanassov, P.; Borup, R. L. *J. Electrochem. Soc.* **2005**, *152*, A1011–A1020.
(39) Yuan, X.-Z.; Zhang, S.; Wang, H.; Wu, J.; Sun, J. C.; Hiesgen, R.; Friedrich, K. A.; Schulze, M.; Haug, A. *J. Power Sources* **2010**, *195*, 7594–7599.
(40) Kabasawa, A.; Uchida, H.; Watanabe, M. *Electrochem. Solid-State Lett.* **2008**, *11*, B190–B192.
(41) Hubner, G.; Roduner, E. *J. Mater. Chem.* **1999**, *9*, 409–418.
(42) Zhang, L.; Mukerjee, S. *J. Electrochem. Soc.* **2006**, *153*, A1062–A1072.